In situ UV/VIS Spectroscopy of Electrochemically Synthesized Selenophene–Thiophene Copolymers

by **Fadi Alakhras**

Department of Chemistry, College of Science, University of Dammam, Dammam 31441, Saudi Arabia (e-mail: falakhras@uod.edu.sa)

Dedicated to Prof. *Muhammad Mubarak* for his impressive ability to impart subject matter to his students. Prof. *Mubarak* taught an entire generation of us to think like scientists. For that, we are all incredibly grateful.

In situ UV/VIS spectroscopy of selenophene–thiophene homo- and copolymer films had been investigated. λ^1_{max} corresponding to the $\pi \rightarrow \pi^*$ interband transition was determined. The optical transition with λ^2_{max} from the valence band into the higher bipolaron band was also allocated. Besides, band gap energy (E_g) of the individual homopolymer and the obtained copolymer films from a direct interband transition was estimated as well, and the values were between 1.91 – 2.10 eV. The influence of applied polymerization potential and monomer feed ratio on the optical properties of the copolymers is discussed.

Introduction. – In recent years, the discovery of doped organic polymers with high conductivities has generated significant research interest among physicists and chemists alike. This type of materials has shown large development concerning the extent of investigated monomers, methods of polymerization and characterization, and suggested applications [1].

Intrinsically conducting polymers obtained from heterocyclic monomers, such as pyrrole or thiophene, have been comprehensively studied over the past two decades. It has been confirmed that characteristics of deposited films are strongly dependent on the electropolymerization conditions. Even though electron conduction occurs through the extended π-bonded system of the polymer backbone, different composition of heteroatoms in similar systems can differ greatly in their electrical properties, chemical stability, and ease of polymerization. The dissimilarity of the heteroatoms was used to adjust the spectro-electrochemical properties, as well as the rigidity of the polymeric backbone.

Polythiophene based polymers are very stable in the oxidized form, which makes these systems one of the most studied conducting polymers. Polythiophenes have been widely studied and have been found excess of applications [2 – 10]. Regardless of the enormous number of reviews published on polythiophenes, relatively less attention was paid on polyselenophenes [11 – 14].

The first preparation of polyselenophenes by electrochemical polymerization was reported in 1983 [15]. The polymer film has a band gap equal to 1.95 eV and the conductivity, in its doped state, of *ca.* 10^{-4} S cm^{-1}. However, the quality of the obtained film was 'not too good'. Consequently, additional efforts to prepare better films were

made in the following years [16–23]. Free-standing polyselenophene polymer films have been effectively synthesized by electrochemical polymerization of selenophene at low potential (E_{SCE} 1.23 V) using $BF_3 \cdot Et_2O$ as solvent system. The polymer shows good mechanical properties with enhanced electrical conductivity to be *ca.* 2.8×10^{-1} S cm^{-1} [24].

During the last decade, a number of selenophene-based copolymers have been synthesized and applied in organic field effect transistors and organic solar cells [25][26]. The main explanations for integrating selenophene monomers into these polymer materials were the expected lower band gap energy due to the lowering of the LUMO and higher hole mobility due to the easily polarized selenophene atom and resulting in strong intermolecular Se·Se interactions [16][24][27][28]. Recently, poly(selenophene-co-thiophene) polymer films have been obtained in our laboratory in two solvent solution systems: MeCN and a binary solvent system consisting of $BF_3 \cdot Et_2O/Et_2O$ (1:2). The redox stability and electrical conductivity of polyselenophene by copolymerization with thiophene monomer units have been remarkably improved [29–31].

Computational studies revealed that polyselenophene material films should have a lower band gap, a more quinoid character, and a more rigid backbone than polythiophenes. Most applications of electrochemical, in particular spectroelectrochemical methods, have aimed at elucidating molecular structural features and electrooptical properties [32].

Accordingly, in the present study it was of interest to elaborate the structure–property relationship of selenophene–thiophene copolymers. The optical properties of the obtained copolymer films were measured using *in situ* UV/VIS spectroscopy and are compared with the pristine homopolymers. The influence of applied polymerization potential and monomer feed ratio on the properties of the copolymers is discussed.

This further attempt to prepare improved copolymer films in terms of redox stability, electrical conductivity, and low band gap energy with alternation of selenophene and thiophene moieties may then represent new types of electrochromic materials.

Results and Discussion. – *Figs. 1* and *2* show the optical absorption spectra changes of polyselenophene and polythiophene recorded *in situ* using UV/VIS spectroscopy during electrochemical p-doping. In the neutral state, polyselenophene shows a broad absorption band at λ^1_{max} *ca.* 507 nm (2.44 eV). This absorption band corresponds to the $\pi \rightarrow \pi^*$ transition, whereby the band's width indicated the coexistence of both long and short effective conjugation lengths in the polymer film [24]. Earlier studies disclosed that the $\pi \rightarrow \pi^*$ absorption peak of selenophene polymer film prepared chemically by dehalogenation from 2,5-dibromoselenophene located at 421 nm [33]. As a rule, the longer wavelength in the spectrum indicates a longer conjugation polymer sequence [34]. Moreover, the redshift of polyselenophene obtained electrochemically from $BF_3 \cdot Et_2O/Et_2O$ (1:2) confirms the high quality and longer conjugation length of as-formed polymer films than those prepared chemically.

The band gap energy of polyselenophene (E_g), which is defined as the difference between the lowest energy in the conduction band and the highest energy in the valence band, can be directly calculated. The band gap energy can be estimated based on the

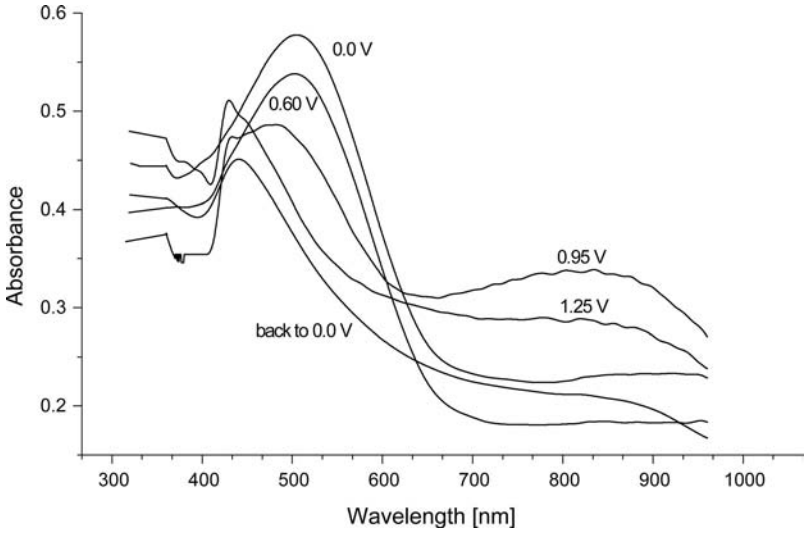

Fig. 1. In situ *UV/VIS spectra recorded at different applied potentials in a solution of MeCN/0.1*M $Bu_4N^+BF_4^-$ *of polyselenophene prepared at* E_{SCE} *1.35 V from* $BF_3 \cdot Et_2O/Et_2O$ (1:2) *solution containing 0.1*M *selenophene and 0.1*M $Bu_4N^+BF_4^-$

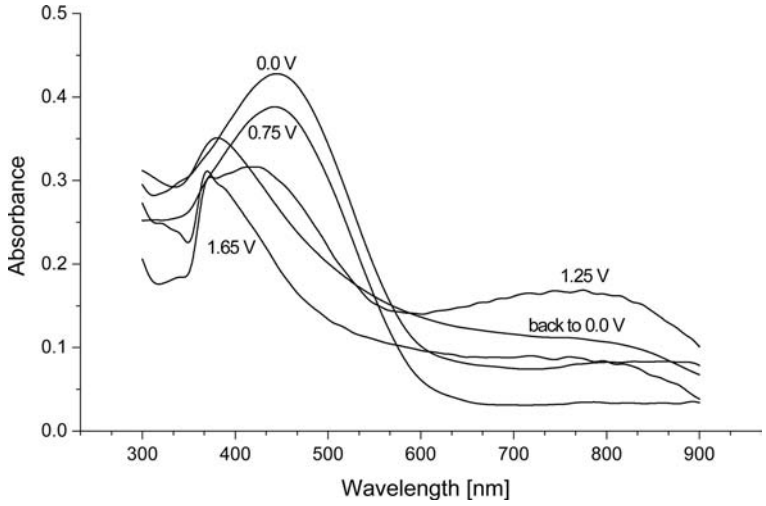

Fig. 2. In situ *UV/VIS spectra recorded at different applied potentials in a solution of MeCN/0.1*M $Bu_4N^+BF_4^-$ *of polythiophene prepared at* E_{SCE} *1.55 V from* $BF_3 \cdot Et_2O/Et_2O$ (1:2) *solution containing 0.1*M *thiophene and 0.1*M $Bu_4N^+BF_4^-$

zero-order approximation [15][23], which is equal to the lowest excitation energy that can be obtained from the onset value at the lower energy edge of the optical absorption spectra. E_g of polyselenophene from a direct interband transition can be evaluated from the absorption edge (*ca.* 650 nm) of the spectrum to be *ca.* 1.91 eV. This value is close to

the reported band gap energy of electropolymerized poly(biselenophene) [35] and polyselenophene [18][36].

When an electron is removed from the top of the valence band of a conjugated polymer, a radical cation is created. Their radical cations are partially delocalized and extended over several monomer units, causing them to deform structurally. These radical cations are called a small polaron. It stabilizes itself by polarizing the medium around it [37][38].

The existence of a polaron over several monomer units can initiate two localized electronic levels in the band gap: a singly occupied bonding polaron state above the valence band edge and an empty antibonding polaron state below the conduction band edge [39]. Additionally, three possible optical transitions below the band gap transition in a slightly doped conjugated polymer can be interpreted as follows: a transition from the valence band to the bonding polaron state, a transition from the bonding to the antibonding polaron state, and the third one matches a transition from the valence band to the antibonding polaron state [40]. Upon further oxidation and at intermediate doping levels, a second electron is removed from the polymer chain and a spinless bipolaron is created. Due to the strong geometry relaxation in the bipolaron case, the polymer sequence becomes more quinoid-like than that with a polaron one. Therefore, the empty bipolaron electronic levels in the band gap get closer to each other than that in the polaron case [41]. Due to the formation of those bipolaron states, two optical transitions can be depicted as follows: the first absorption can be related to a transition from the valence band to the lower bipolaron level and the second one from the valence band to the upper bipolaron level. The bipolaron states at high dopant concentration overlap and form two wide bands in the gap which has been taken from the valence and conduction band edges. Nevertheless, for a hypothetical 100% doping level, theoretical calculations indicate that the lower (upper) bipolaron band merges with the valence band (conduction band). Consequently, the gap between the valence and conduction band edges almost decreases suggesting metallic-like behavior.

Upon doping and when a potential of $+0.95$ V was applied, the interband transition almost vanished; however, a very broad characteristic appeared with its maximum shifting into NIR upon further oxidation. The optical transition with λ^2_{max} from the valence band into the higher bipolaron band (the higher subgap state) was located at 817 nm (1.51 eV). The original band gap of polyselenophene increased from 1.91 eV in the neutral state to 2.10 eV in the doped state (*Fig. 3*). These remarkable changes are typical characteristics of conducting polymers, and this assignment was previously reported [24][35].

Polythiophene showed a single absorption peak at 2.77 eV in its neutral state which is consistent with published work [42][43]. This broad λ^1_{max} assigned to the $\pi \rightarrow \pi^*$ interband transition. Upon oxidation to 1.25 V, the peak height of the interband transition was diminished, and another broad absorption band λ^2_{max} appeared simultaneously at *ca.* 775 nm (1.64 eV). These spectral changes may be explained in terms of removing electrons from the valence band and the formation of polaron/bipolaron states upon electrochemical doping.

In the band gap, two bipolaron energy states/bands were formed, and the upper one was located at 0.46 eV below the conduction band. The band gap was also widened from 2.10 eV in the neutral state to 2.32 eV in the electrochemically doped state (*Fig. 3*).

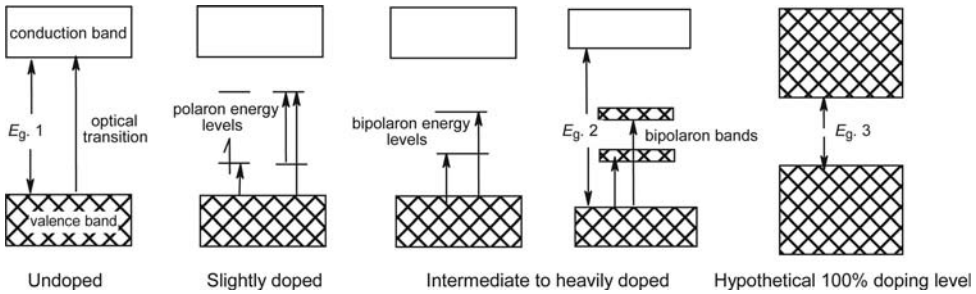

Fig. 3. *Polaron, bipolaron energy levels, conduction, valence, bipolaron bands, as well as optical transitions in homopolymers.* E_g. 1: Band gap of neutral polymer, E_g. 2: band gap of intermediate to heavily doped polymer, E_g. 3: band gap of hypothetical 100% doping level.

The absorption bands and band gaps of polyselenophene and polythiophene are listed in *Table 1*.

In situ UV/VIS spectra both at different electrode potentials and with different monomer feed ratio in the polymerization solution were investigated. *Fig. 4,a–4,c* shows the *in situ* UV/VIS spectra of the copolymers obtained from $BF_3 \cdot Et_2O/Et_2O$ (1:2) solution containing 0.10M selenophene and 0.10M thiophene at potentials ranging from E_{SCE} 1.4 to 1.6 V, respectively.

The copolymers represented a broad absorption band in the neutral state. This λ^1_{max} attributed to the $\pi \rightarrow \pi^*$ interband transition, demonstrating that both of long and short effective conjugated lengths containing selenophene and thiophene monomer units coexisted along the copolymer chains. Furthermore, upon increasing the polymerization potential of the copolymers, a blueshift of the absorption band in the neutral state was observed.

When the copolymer was prepared at E_{SCE} 1.4 V, its spectra showed interband transition at 485 nm, whereas the copolymer obtained at E_{SCE} 1.6 V showed at λ^1_{max} 463 nm, which was closer to pure polythiophene absorption band. This indicated that more thiophene units were incorporated into the copolymer chains with an increase of the preparation potential.

Upon electrochemical p-doping, the same behavior was still observed. The interband transition nearly disappeared, and a very broad characteristic appeared (λ^2_{max}) instead of its maximum shifting into NIR upon further oxidation. This feature can be attributed to the formation of polaron/bipolaron transitions between band gap states, which arose as a consequence of electronic coupling with the polymer backbone. Conceivable polaron and bipolaron structures in the copolymers are shown in *Fig. 5*.

Table 1. *Absorption Bands and Band Gaps of Polyselenophene and Polythiophene*

Homopolymer	λ^1_{max}		λ^1_{max}		Band gap	
	[nm]	[eV]	[nm]	[eV]	[nm]	[eV]
Polyselenophene	507	2.44	817	1.51	650	1.91
Polythiophene	447	2.77	757	1.64	590	2.10

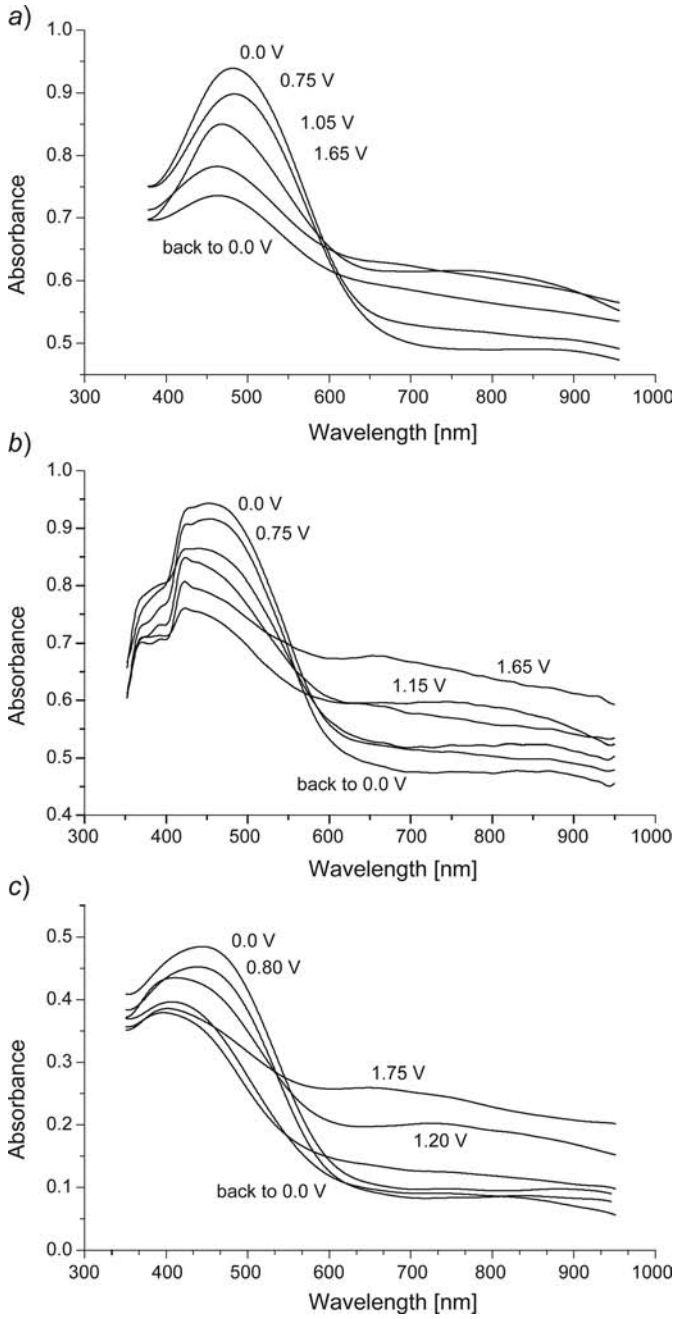

Fig. 4. In situ *UV/VIS spectra recorded at different applied potentials in a solution of MeCN/0.1*M $Bu_4N^+BF_4^-$ *of copolymers prepared at* E_{SCE} *1.4 V* (*a*), *1.5 V* (*b*), *1.6 V* (*c*) *from* $BF_3 \cdot Et_2O/Et_2O$ (1:2) *solution containing 0.1*M *selenophene, 0.1*M *thiophene, and 0.1*M $Bu_4N^+BF_4^-$

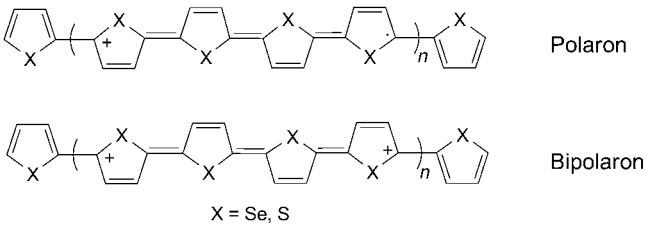

Fig. 5. *Conceivable polaron and bipolaron structures in obtained copolymers*

The band gap energies of copolymers obtained at preparation potentials ranging from E_{SCE} 1.4 to 1.6 V from a direct interband transition can also be calculated from the absorption edge of the spectrum. When the polymerization potential was increased, a hypsochromic shift (*ca.* 630–619 nm) resulted, and the band gap values were between 1.97 and 2.00 eV, respectively. The absorption bands and band gaps of copolymers obtained from $BF_3 \cdot Et_2O/Et_2O$ (1:2) solution containing 0.10M selenophene and 0.10M thiophene at potentials ranging from E_{SCE} 1.4 to 1.6 V are listed in *Table 2*.

When the monomer feed ratio was changed from 1:1 to 3:1 and to 6:1, the *in situ* UV/VIS spectra were recorded as well (*Fig. 6*). The same existing features were still observed: broad λ^1_{max} assigned to the $\pi \rightarrow \pi^*$ interband transition, which almost vanished, and as an alternative, a very broad λ^2_{max} appeared with its maximum shifting into NIR upon further oxidation. In addition, a higher concentration of selenophene in the feed led to a bathochromic shift of the interband transition of the copolymer obtained. It was clearly observable that the copolymer film electro-synthesized in a solution containing selenophene/thiophene (1:1) polymerized at E_{SCE} 1.5 V showed λ^1_{max} at 472 nm, while a copolymer obtained in a solution containing selenophene/thiophene (6:1) showed an absorption band around 493 nm. The absorption bands and band gaps of the copolymers prepared at different polymerization potentials from these different solutions are listed in *Table 3* and *4*.

Depending on the above results, we may conclude that, at higher polymerization potentials and at higher concentrations of thiophene in the polymerization solution, more thiophene units are integrated into the copolymer chains. Additionally, the band gap energies of the obtained copolymers are between those of the individual homopolymers. This implies that the oxidation of monomers is feasible, and the obtained films are composed of both selenophene and thiophene units [29–31], which may eliminate the opportunity of having block copolymers [42]. The film deposited at

Table 2. *Absorption Bands and Band Gaps of Copolymers Obtained from $BF_3 \cdot Et_2O/Et_2O$ (1:2) Solutions Containing 0.10M Selenophene and 0.10M Thiophene at Potentials Ranging from E_{SCE} 1.4 to 1.6 V*

Polymerization potential	λ^1_{max}		λ^2_{max}		Band gap	
	[nm]	[eV]	[nm]	[eV]	[nm]	[eV]
1.4	485	2.56	796	1.56	630	1.97
1.5	472	2.63	781	1.59	623	1.99
1.6	463	2.68	762	1.63	619	2.00

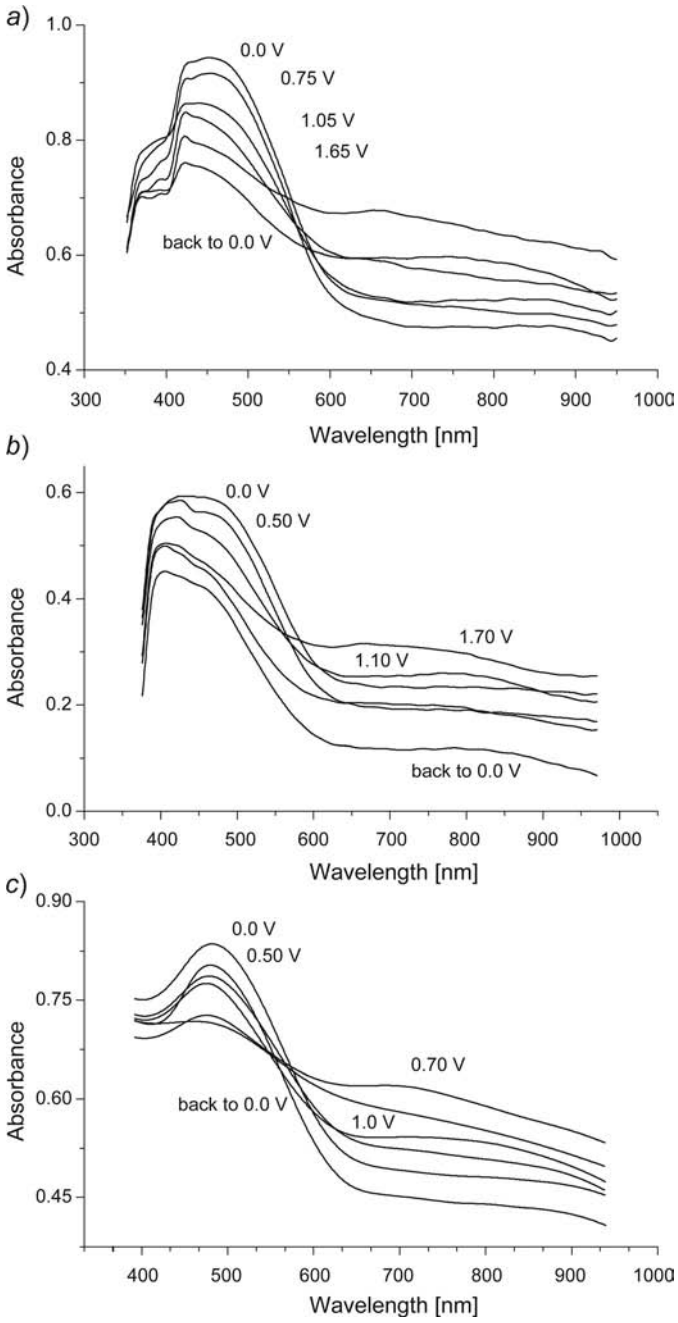

Fig. 6. In situ *UV/VIS spectra recorded at different applied potentials in a solution of MeCN/0.1*M $Bu_4N^+BF_4^-$ *of copolymers prepared at* E_{SCE} *1.5 V from different solutions containing selenophene/thiophene 1:1* (*a*), *3:1* (*b*), *6:1* (*c*) *in the presence of 0.1*M $Bu_4N^+BF_4^-$

Table 3. *Absorption Bands and Band Gaps of Copolymers Obtained from $BF_3 \cdot Et_2O/Et_2O$* (1:2) *Solution Containing Selenophene/Thiophene* (3:1) *at Potentials Ranging from* E_{SCE} *1.4 to 1.6 V*

Polymerization potential	λ^1_{max}		λ^2_{max}		Band gap	
	[nm]	[eV]	[nm]	[eV]	[nm]	[eV]
1.4	495	2.50	806	1.54	637	1.95
1.5	490	2.53	788	1.57	631	1.96
1.6	480	2.58	768	1.61	626	1.98

Table 4. *Absorption Bands and Band Gaps of Copolymers Obtained from $BF_3 \cdot Et_2O/Et_2O$* (1:2) *Solution Containing Selenophene/Thiophene* (6:1) *at Potentials Ranging from* E_{SCE} *1.4 to 1.6 V*

Polymerization potential	λ^1_{max}		λ^2_{max}		Band gap	
	[nm]	[eV]	[nm]	[eV]	[nm]	[eV]
1.4	500	2.48	814	1.52	642	1.93
1.5	493	2.51	795	1.56	638	1.94
1.6	485	2.56	774	1.60	633	1.96

E_{SCE} 1.6 V with feed ratio 1:1 may comprise structure close to those of polythiophene-based random copolymer films, whilst the film obtained at E_{SCE} 1.4 V with feed ratio 6:1 may be regarded as polyselenophene-based random material films.

Upon reduction, the initial spectrum of homo- and copolymer films was not re-established completely. This indicated that some irreversible process occurred during oxidation/reduction of the films. This behavior is commonly observed in conducting polymers, which is related to partial destruction of conjugated structures in the polymer chains [44][45].

Conclusions. – The electrosynthesis of selenophene and thiophene homo- and copolymer films has been carried out in a binary solvent system consisting of $BF_3 \cdot Et_2O/Et_2O$ (1:2). The optical properties of these material films were investigated using *in situ* UV/VIS spectroscopy. The interband $\pi \rightarrow \pi^*$ transition nearly disappeared and, however, a very broad characteristic appeared (λ^2_{max}) with its maximum shifting into NIR upon further oxidation. This feature can be attributed to the formation of polaron/bipolaron transitions between band gap states, which arise as a consequence of electronic coupling with the polymer backbone. The spectra of the copolymers revealed intermediate optical properties between those of homopolymers. Furthermore, at higher polymerization potentials and at higher concentrations of thiophene in the polymerization solution, more thiophene units are integrated into the copolymer chains.

The author wishes to acknowledge the University of Dammam for financial support.

Experimental Part

General. Selenophene (98%; *TCI*) and thiophene (99%; *Acros*) were distilled under N_2 just prior to use. Et_2O (*Fisher Scientific*) was dried and distilled in the presence of Na. $BF_3 \cdot Et_2O$ (48% BF_3, *Acros*) was used as received. $Bu_4N^+BF_4^-$ (98%; *Acros*) was dried under vacuum at 80° for 24 h. MeCN (anh., < 10 ppm H_2O; *Merck*) was used without further purification.

The electrochemical polymerizations between selenophene and thiophene were carried out in a one-compartment three-electrode cell by using a 150 potentiostat/galvanostat (*Bio-Logic*) under computer control (*EC-Lab*) software. A platinum disc electrode was used as working electrode for electrosynthesis and CV measurements; whereas ITO coated glass electrodes were used as working electrodes for *in situ* UV/VIS spectroscopy. Saturated calomel electrode (SCE) was used as reference electrode.

The electrosynthesis was carried out potentiostatically in $BF_3 \cdot Et_2O/Et_2O$ 1:2 soln., containing in addition 0.1M $Bu_4N^+BF_4^-$ as supporting electrolyte, at r.t. at constant electrode potential for 2 min. After polymerization, the film was washed with MeCN to remove any traces of mono- and oligomers. All solns. were deaerated by a dry N_2 stream for 10 min before the experiment and a slight N_2 over-pressure was maintained during the experiment.

UV/VIS Spectra were recorded for the obtained homo- and copolymer films in a standard 10 mm cuvette containing the supporting electrolyte soln. using a *Shimadzu UV 1800-PC* instrument (resolution 1 nm); a cuvette with the same soln. and uncoated ITO glass was placed in the reference beam. The CVs of homo- and copolymer films are provided in *Fig. 7* to determine the suitable range of electrode potentials for UV/VIS experiments (for further details see [30]). The absorption maximum λ^1_{max} assigned

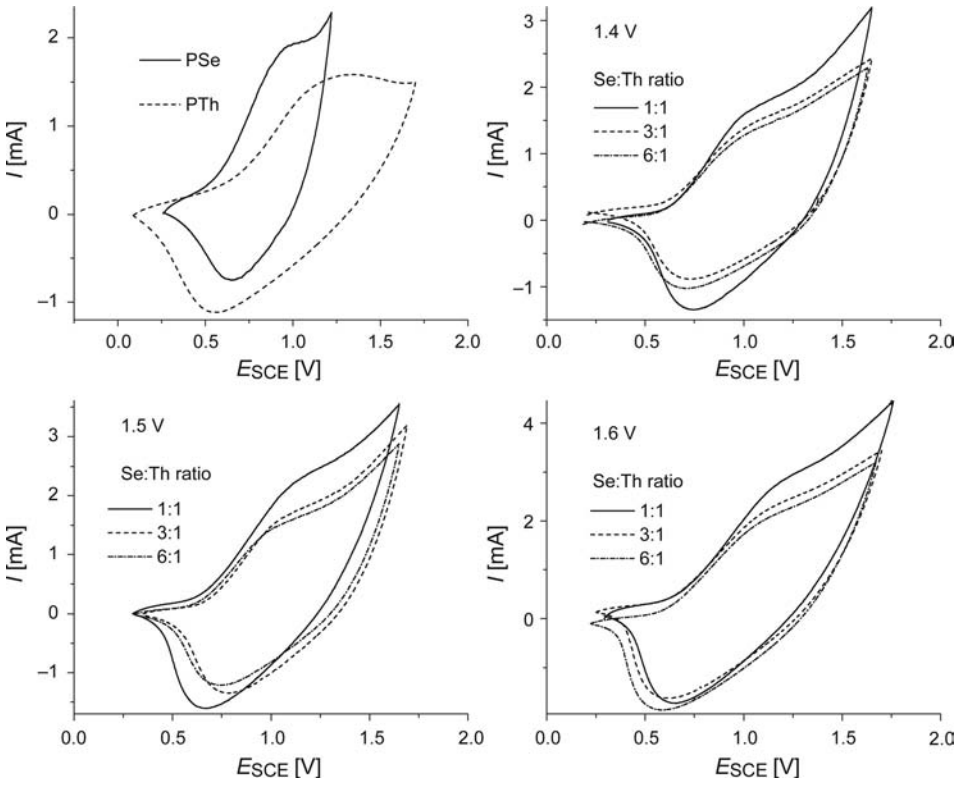

Fig. 7. *CVs Recorded in MeCN/0.10M $Bu_4N^+BF_4^-$ solution of homo- and copolymer films obtained from $BF_3 \cdot Et_2O/Et_2O$ (1:2) solution.* $dE/dt = 100$ mV/s.

to the $\pi \rightarrow \pi^*$ transition was measured with the polymer in its neutral state, whereas the absorption maximum λ^2_{max} assigned to an intraband transition from the valence band into the upper bipolaron band of the polymer was conducted in its oxidized form.

REFERENCES

[1] R. Holze, 'Handbook of Advanced Electronic and Photonic Materials and Devices', Academic Press, San Diego, 2001; R. Holze, 'Advanced Functional Molecules and Polymers', Gordon & Breach, Amsterdam, 2001.
[2] D. Kelkar, A. Chourasia, *Chem. Chem. Technol*. **2011**, *5*, 309.
[3] A. Malinauskas, *Synth. Met*. **1999**, *107*, 75.
[4] G. Grundmeier, W. Schmidt, M. Stretmann, *Electrochim. Acta* **2000**, *45*, 2515.
[5] K. Gurunathan, A. V. Mrurgan, R. Marimuthu, U. P. Mulik, D. P. Amalnerkar, *Mater. Chem. Phys.* **1999**, *61*, 173.
[6] T. F. Otero, I. Cantero, *Power Sources* **1999**, *81*, 838.
[7] F. Beck, P. Rüetschi, *Electrochim. Acta* **2000**, *45*, 2467.
[8] R. S. Bobade, *J. Polym. Eng.* **2011**, *31*, 209.
[9] S. Cosnier, *Biosen. Bioelectron*. **1999**, *14*, 443.
[10] R. V. Parthasarathy, C. R. Martin, *Nature* **1994**, *369*, 298.
[11] A. Berlin, G. Zotti, S. Zecchin, G. Schiavon, M. Cocchi, D. Virgili, C. Sabatini, *J. Mater. Chem*. **2003**, *13*, 27.
[12] S. Glenis, M. Benz, E. LeGoff, J. L. Schindler, C. R. Kanewurf, M. G. Kanatzidis, *J. Am. Chem. Soc*. **1993**, *115*, 12519.
[13] A. R. Hillman, E. F. Mallen, *J. Electroanal. Chem. Interfacial Electrochem.* **1990**, *281*, 109.
[14] S. Hasoon, M. Galtier, J. L. Sauvajol, J. P. Lère-Porte, A. Bonniol, B. Moukala, *Synth. Met*. **1989**, *28*, 317.
[15] K. Yoshino, K. Kaneto, S. Inoue, K. Tsukagoshi, *Jpn. J. Appl. Phys.* **1983**, *22*, L701.
[16] A. Patra, M. Bendikov, *J. Mater. Chem*. **2010**, *20*, 422.
[17] Y. Narita, I. Hagiri, N. Takahashi, K. Takeda, *Jpn. J. Appl. Phys.* **2004**, *43*, 4248.
[18] U. Salzner, J. B. Lagowski, P. G. Pickup, R. A. Poirier, *Synth. Met*. **1998**, *96*, 177.
[19] S. Inoue, H. Nakanishi, K. Takimiya, Y. Aso, T. Otsubo, *Synth. Met*. **1997**, *84*, 341.
[20] C. Wang, A. Ellern, J. Y. Becker, J. Bernstein, *Adv. Mater*. **1995**, *7*, 644.
[21] M. A. del Valle, L. Ugalde, F. R. Diaz, M. E. Bodini, J. C. Bernède, A. Chaillou, *Polym. Bull*. **2003**, *51*, 55.
[22] J. L. Sauvajol, D. Chenouni, S. Hasoon, J. P. Lère-Porte, *Synth. Met*. **1989**, *28*, 293.
[23] S. Glenis, D. S. Ginley, A. J. Frank, *J. Appl. Phys.* **1987**, *62*, 190.
[24] J. Xu, J. Hou, S. Zhang, G. Nie, S. Pu, L. Shen, Q. Xiao, *J. Electroanal. Chem*. **2005**, *587*, 345.
[25] H. Kong, D. S. Chung, I.-N. Kang, J.-H. Park, M.-J. Park, I. H. Jung, C. E. Park, H.-K. Shim, *J. Mater. Chem*. **2009**, *19*, 3490.
[26] W.-H. Lee, S. K. Lee, S. K. Son, J.-E. Choi, W. S. Shin, K. Kim, S.-H. Lee, S.-J. Moon, I.-N. Kang, *J. Polym. Sci., Part A: Polym. Chem.* **2012**, *50*, 551.
[27] M. D. Bezoari, P. Kovacic, S. Gronowitz, A.-B. Hörnfeldt, *J. Polym. Sci., Polym. Lett. Ed*. **1981**, *19*, 347.
[28] E. Aqad, M. V. Lakshmikantham, M. P. Cava, *Org. Lett*. **2001**, *3*, 4283.
[29] F. Alakhras, *Mater. Sci. Poland* **2015**, *33*, 25.
[30] F. Alakhras, *Chem. Chem. Technol*. **2014**, *8*, 265.
[31] F. Alakhras, *Arab. J. Sci. Eng*. **2014**, DOI 10.1007/s13369-014-1514-8.
[32] J. Arjomandi, F. Alakhras, W. Al-Halasah, R. Holze, *Jordan J. Chem.* **2009**, *4*, 279.
[33] K. Kizu, T. Maruyama, T. Yamamoto, *Polym. J*. **1995**, *27*, 205.
[34] S. Pu, J. Hou, J. Xu, G. Nie, S. Zhang, L. Shen, Q. Xiao, *Mater. Lett*. **2005**, *59*, 1061.
[35] T.-T. Ong, S.-C. Ng, H. S. O. Chan, *Polymer* **2003**, *44*, 5597.
[36] N. Marcal, B. Laks, *Int. J. Quantum Chem*. **2003**, *95*, 230.
[37] J. C. Scott, P. Pfluger, M. T. Krounbi, G. B. Street, *Phys. Rev. B* **1983**, *28*, 2140.

[38] W. P. Su, J. R. Schrieffer, A. J. Heeger, *Phys. Rev. Lett*. **1979**, *42*, 1698.
[39] J. L. Bredas, J. C. Scott, K. Yakushi, G. B. Street, *Phys. Rev. B* **1984**, *30*, 1023.
[40] J. L. Bredas, B. Thémans, J. G. Fripiat, J. M. André, R. R. Chance, *Phys. Rev. B* **1984**, *29*, 6761.
[41] J. L. Bredas, G. B. Street, *Acc. Chem. Res.* **1985**, *18*, 309.
[42] F. Alakhras, R. Holze, *Synth. Met*. **2007**, *157*, 109.
[43] F. Alakhras, R. Holze, *J. Solid State Electrochem*. **2008**, *12*, 81.
[44] S. Vogel, R. Holze, *Electrochim. Acta* **2005**, *50*, 1587.
[45] G. Inzelt, M. Pineri, J. W. Schultze, M. A. Vorotyntsev, *Electrochim. Acta* **2000**, *45*, 2403.

Received November 20, 2014